J|A|C|S ARTICLES

Published on Web 09/16/2009

Synthesis, Stability, and Photochemistry of Pentacene, Hexacene, and Heptacene: A Matrix Isolation Study

Rajib Mondal,[†,‡,⊥] Christina Tönshoff,[†,§] Dmitriy Khon,[‡] Douglas C. Neckers,[‡] and Holger F. Bettinger*[,†,§]

Lehrstuhl für Organische Chemie II, Ruhr-Universität Bochum, Universitätsstrasse 150, 44780 Bochum, Germany, Center for Photochemical Sciences, Bowling Green State University, Bowling Green, Ohio 43403, and Institut für Organische Chemie, Universität Tübingen, Auf der Morgenstelle 18, 72076 Tübingen, Germany

Received March 15, 2009; E-mail: Holger.Bettinger@uni-tuebingen.de

Abstract: The photochemical bisdecarbonylation of bridged α-diketones (Strating−Zwanenburg reaction) to give the oligoacenes pentacene (**2**), hexacene (**3**), and heptacene (**4**) is investigated in solid inert gas matrices at cryogenic temperatures. The photodecomposition using visible light irradiation cleanly produces the corresponding oligoacene without formation of observable intermediates. This synthetic approach to the higher acenes allows a comprehensive comparative study of their electronic absorption and infrared spectral properties under identical conditions for the first time. In addition, the route makes it possible to investigate the thermal and photochemical stability of these higher acenes and addresses the problem of heptacene stability which dates back almost 70 years. This largest known member of the acene series is found to be unstable at room temperature. Furthermore, all oligoacenes **2**−**4** undergo a photoredox reaction upon 185 nm excitation, resulting in the concurrent formation of radical cations and anions in the noble gas matrix. These polaron states of the oligoacenes are stable under the conditions of their generation but collapse to the uncharged acenes upon visible light irradiation.

Introduction

The acenes **1** (Chart 1), polycyclic aromatic hydrocarbons (PAH) composed of linearly annelated benzene units, have fascinated organic chemists for more than a century.[1−5] Research in PAH chemistry in general, and acenes in particular, has experienced a surge during the last decades, as these hydrocarbons are of importance in such diverse fields such as materials and nanoscience, theoretical organic chemistry, and astrochemistry.[2−5] PAHs are central to efforts aimed at quantifying the concept of aromaticity,[6] can be considered as building blocks of carbonaceous materials such as graphene[7,8] and carbon nanotubes,[9,10] and have been suggested to be carriers of the unidentified IR emission (more recently known as aromatic IR bands, AIBs) and the diffuse interstellar bands (DIBs).[11−15]

Chart 1. Structures of Polyacene **1** and the Higher Acenes, Pentacene (**2**), Hexacene (**3**), and Heptacene (**4**), Investigated in the Present Work

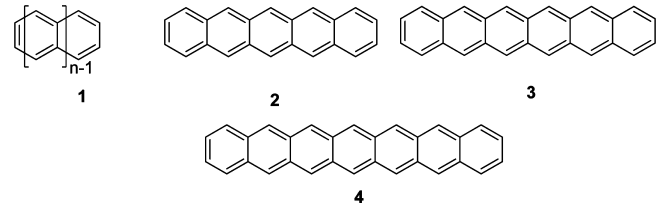

The considerable interest in acenes from an organic electronic materials perspective is caused by their unique electronic structure that has been the subject of numerous theoretical investigations.[16−30] The topology of their π electron systems

† Ruhr-Universität Bochum.
‡ Bowling Green State University.
§ Universität Tübingen.
⊥ Present address: Department of Chemical Engineering, Stanford University, Stanford, CA 94085.

(1) Clar, E. *Polycyclic Hydrocarbons*; Academic Press: New York, 1964; Vol. 1.
(2) Anthony, J. E. *Chem. Rev.* **2006**, *106*, 5028.
(3) Anthony, J. E. *Angew. Chem., Int. Ed.* **2008**, *47*, 452.
(4) Bendikov, M.; Wudl, F.; Perepichka, D. F. *Chem. Rev.* **2004**, *104*, 4891.
(5) Würthner, F.; Schmidt, R. *ChemPhysChem* **2006**, *7*, 793.
(6) Schleyer, P. v. R.; Manoharan, M.; Jiao, H.; Stahl, F. *Org. Lett.* **2001**, *3*, 3643.
(7) Novoselov, K. S.; Geim, A. K.; Morozov, S. V.; Jiang, D.; Zhang, Y.; Dubonos, S. V.; Grigorieva, I. V.; Firsov, A. A. *Science* **2004**, *306*, 666.
(8) Geim, A. K.; Novoselov, K. S. *Nat. Mater.* **2007**, *6*, 183.
(9) Dresselhaus, M. S.; Dresselhaus, G.; Eklund, P. C. *Science of Fullerenes and Carbon Nanotubes*; Academic Press: San Diego, 1996.
(10) Dresselhaus, M. S.; Dresselhaus, G.; Avouris, P., Eds. *Carbon Nanotubes*; Springer: Berlin, 2001.
(11) Léger, A.; Puget, J. L. *Astron. Astrophys.* **1984**, *137*, L5.
(12) Allamandola, L. J.; Tielens, A. G. G. M.; Barker, J. R. *Astrophys. J.* **1985**, *290*, L25.
(13) Crawford, M. K.; Tielens, A. G. G. M.; Allamandola, L. J. *Astrophys. J.* **1985**, *293*, L45.
(14) Van der Zwet, G. P.; Allamandola, L. J. *Astron. Astrophys.* **1985**, *146*, 76.
(15) Léger, A.; d'Hendecourt, L. *Astron. Astrophys.* **1985**, *146*, 81.
(16) Coulson, C. A. *Proc. Phys. Soc. London* **1948**, *60*, 257.
(17) Tavan, P.; Schulten, K. *J. Chem. Phys.* **1979**, *70*, 5414.
(18) Wiberg, K. B. *J. Org. Chem.* **1997**, *62*, 5720.
(19) Kawashima, Y.; Hashimoto, T.; Nakano, H.; Hirao, K. *Theor. Chem. Acc.* **1999**, *102*, 49.
(20) Heinze, H. H.; Görling, A.; Rösch, N. *J. Chem. Phys.* **2000**, *113*, 2088.

results in HOMO−LUMO energy gaps that are smaller than for other hydrocarbons with a similar number of aromatic rings.[1] The energy gap quickly decreases with the length of the conjugated π system, as seen in the bathochromic shift of the absorption spectra[1] and the decreasing singlet−triplet energy splitting.[27] This has two decisive and interrelated consequences: the acenes are turning from insulators to organic molecular p-type semiconductors with increasing length, and at the same time they turn from prototypical stable aromatic compounds to reactive species.[31] The decrease in the reorganization energies,[32] the increase in the charge carrier mobilities, and the band widths make tetracene and the higher acenes useful materials for organic electronic applications.[2−5,33−35] Because of the quickly increasing reactivity of acenes, only the members up to the size of pentacene are characterized well. Hexacene already slowly decomposes in solution at room temperature.[36] The existence of heptacene was controversial since the 1942 report by Clar,[37] as repeated synthetic attempts at heptacene failed until 2006. The lack of experimental information on the thermal stability of heptacene led to several reinvestigations of the synthesis, and the common conclusion was that heptacene appears to be the limiting acene with respect to stability.[37−40] Though kinetically stabilized heptacene derivatives were obtained in 2005 by Payne et al.[41] and very recently by Chun et al.[42] and Kaur et al.,[43] the synthesis of the parent heptacene was only reported recently and required the use of stabilizing matrices.[44,45] However, an analysis of its IR and electronic absorption spectra is lacking and no information is available on its singly charged radical ions.

The successful syntheses of the reactive higher parent acenes relied on the photochemical bisdecarbonylation, known as the Strating−Zwanenburg[46] reaction, of bridged α-diketones (**5**−**7**).[36,44,45,47] These compounds have two advantages in acene synthesis: they are reasonably soluble in organic solvents, and photolysis can be used efficiently in matrix isolation experiments.[45] As reported here, the utilization of the Strating−Zwanenburg reaction allowed us to investigate and compare the thermal stabilities, spectral properties, and the photoinduced radical ion formation of the three largest known acenes, pentacene (**2**), hexacene (**3**), and heptacene (**4**), under identical conditions for the first time (Scheme 1).

Scheme 1. Photogeneration of Higher Acenes **2**−**4** from the Diketones **5**−**7** and Photochemically Induced Charge Transfer To Yield the Acene Radical Anions and Radical Cations Investigated in the Present Work

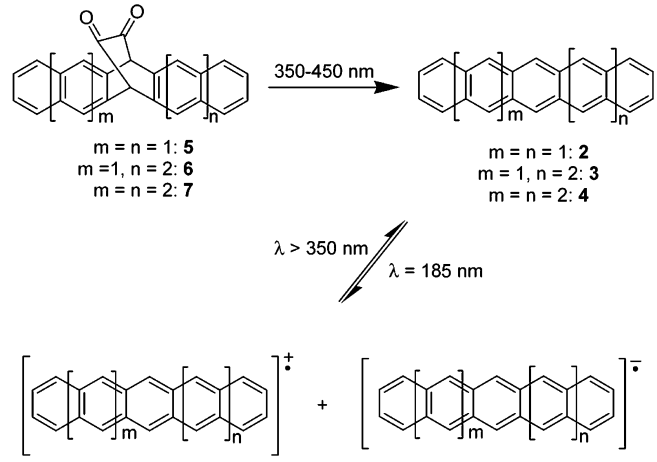

Experimental Section

The α-diketones (**5**−**7**) were synthesized as described previously.[36,44,47] Matrix isolation experiments were carried out according to standard techniques[48] with APD CSW-20 displex closed-cycle helium cryostats. The photoprecursors (**5**−**7**) were sublimed out of a quartz tube that was resistively heated by a tantalum coil to 163−170 °C, 193−198 °C, and 220−227 °C, respectively. As the UV/vis spectrum of tetracene in argon is not available, this was measured by subliming tetracene (Aldrich, 98%) at 75−80 °C (see Supporting Information, Figure S1). The gaseous materials were trapped onto cold CsI (IR experiments) or sapphire spectroscopic windows with a large excess of argon (Messer Griesheim, 99.9999%) or xenon (Air Liquide, 4.0) gas that were dosed to 2.0 sccm by a mass flow controller (MKS Mass Flo type 247 four-channel read out). The experiments performed in xenon are not discussed further here for the sake of conciseness. The windows were kept at 30 and 55 K during deposition of argon and xenon, respectively, by resistive heating using an Oxford ITC 503 temperature controller. Photolysis of the diketones and the photogenerated acenes were carried out using a high-pressure mercury lamp equipped with 350−450 nm mirror and a low pressure mercury lamp (Gräntzel lamp) that irradiates 185 and 254 nm wavelength light. IR spectra were measured on Bruker IFS 66 and IFS 66/S spectrometers using a resolution of 0.5 cm^{-1}, while electronic absorption spectra were measured using a Cary 5000 spectrometer.

(21) Houk, K. N.; Lee, P. S.; Nendel, M. *J. Org. Chem.* **2001**, *66*, 5517.
(22) Marian, C. M.; Gilka, N. *J. Chem. Theory Comput.* **2008**, *4*, 1501.
(23) Grimme, S.; Parac, M. *ChemPhysChem* **2003**, *4*, 292.
(24) Bendikov, M.; Duong, H. M.; Starkey, K.; Houk, K. N.; Carter, E. A.; Wudl, F. *J. Am. Chem. Soc.* **2004**, *126*, 7416.
(25) Kadantsev, E. S.; Stott, M. J.; Rubio, A. *J. Chem. Phys.* **2006**, *124*, 134901.
(26) Sony, P.; Shukla, A. *Phys. Rev. B* **2007**, *75*, 155208.
(27) Hachmann, J.; Dorando, J. J.; Avilés, M.; Chan, G. K.-L. *J. Chem. Phys.* **2007**, *127*, 134309.
(28) Malloci, G.; Mulas, G.; Cappellini, G.; Joblin, C. *Chem. Phys.* **2007**, *340*, 43.
(29) Jiang, D.; Dai, S. *J. Phys. Chem. A* **2008**, *112*, 332.
(30) Qu, Z.; Zhang, D.; Liu, C.; Jiang, Y. *J. Phys. Chem. A* **2009**, *113*, 7909.
(31) Biermann, D.; Schmidt, W. *J. Am. Chem. Soc.* **1980**, *102*, 3163.
(32) Winkler, M.; Houk, K. N. *J. Am. Chem. Soc.* **2007**, *129*, 1805.
(33) Würthner, F. *Angew. Chem., Int. Ed.* **2001**, *40*, 1037.
(34) Dimitrakopoulos, C. D.; Malenfant, P. R. L. *Adv. Mater.* **2002**, *14*, 99.
(35) Kitamura, M.; Arakawa, Y. *J. Phys.: Condens. Matter* **2008**, *20*, 184011.
(36) Mondal, R.; Adhikari, R. M.; Shah, B. K.; Neckers, D. C. *Org. Lett.* **2007**, *9*, 2505.
(37) Clar, E. *Chem. Ber.* **1942**, *75*, 1330.
(38) Bailey, W. J.; Liao, C.-W. *J. Am. Chem. Soc.* **1955**, *77*, 992.
(39) Marschalk, C. *Bull. Soc. Chim.* **1943**, *10*, 511.
(40) Boggiano, B.; Clar, E. *J. Chem. Soc.* **1957**, 2681.
(41) Payne, M. M.; Parkin, S. R.; Anthony, J. E. *J. Am. Chem. Soc.* **2005**, *127*, 8028.
(42) Chun, D.; Cheng, Y.; Wudl, F. *Angew. Chem., Int. Ed.* **2008**, *47*, 8380.
(43) Kaur, I.; Stein, N. N.; Kopreski, R. P.; Miller, G. P. *J. Am. Chem. Soc.* **2009**, *131*, 3424.
(44) Mondal, R.; Shah, B. K.; Neckers, D. C. *J. Am. Chem. Soc.* **2006**, *128*, 9612.
(45) Bettinger, H. F.; Mondal, R.; Neckers, D. C. *Chem. Commun.* **2007**, 5209.
(46) Strating, J.; Zwanenburg, B.; Wagenaar, A.; Udding, A. C. *Tetrahedron Lett.* **1969**, 125.
(47) Yamada, H.; Yamashita, Y.; Kikuchi, M.; Watanabe, H.; Okujima, T.; Uno, H.; Ogawa, T.; Ohara, K.; Ono, N. *Chem.—Eur. J.* **2005**, *11*, 6212.
(48) Dunkin, I. R. *Matrix-Isolation Techniques*; Oxford University Press: Oxford, 1998.

The computational investigations used the B3LYP[49,50] hybrid functional as implemented in Gaussian 03[51] for the optimization of the geometry and computation of harmonic vibrational frequencies of acenes and their singly charged radical ions in conjunction with the 6-31G* basis set. A scaling factor of 0.985 was employed for the vibrational frequencies as recommended.[52] Electronic excitations of acene radical ions were computed using time-dependent B3LYP (TD-B3LYP) in conjunction with the 6-31G* basis set. Excited states of acenes were also computed at the RICC2/TZVPP level of theory, see Supporting Information for details. The axis system used is: *x*, long axis; *y*, short axis; *z*, out-of-plane axis.

Results and Discussion

A. Photosynthesis of Higher Acenes from α-Diketones 5−7. Isolation of the α-diketones (**5**−**7**) in inert gas matrices is achieved by heating a sample to approximately 170, 195, and 225 °C, respectively, at a pressure of $\sim 10^{-5}$ mbar and condensing with a large excess of inert gas. As expected, the α-diketones show similar IR and UV spectral properties (see Supporting Information, Tables S1 and S2). The most characteristic feature of these compounds in the IR spectral region are the carbonyl stretching vibrations, which give rise to a structured band extending from 1716 to 1770 cm^{-1}. The n → π* transitions are features which display some vibrational fine structure and extend from 440 up to about 500 nm. The strong β band of the naphthalene subunit is observed at 234 nm for **5**. This shifts to 269 nm for **7**, which is composed of two anthracene subunits. The unsymmetrical diketone **6**, on the other hand, shows two bands of similar intensity at 250 and 263 nm.

All α-diketones behave similarly upon irradiation with a high-pressure mercury lamp ($385 < \lambda < 450$ nm): all the mid-IR and UV/vis bands decrease during irradiation, and extended photolysis results in essentially complete disappearance of **5**−**7**. During irradiation, the expected signals of CO in the IR (2138 cm^{-1}, 2137 cm^{-1}, and 2133 cm^{-1} due to monomeric CO and aggregated CO)[53] are being formed along with signals that are assigned to the desired acenes (vide infra). In neither case could we detect any photolabile intermediates by IR or UV/vis spectroscopy. Rather, following the photochemical decomposition of **5**−**7** by UV/vis spectroscopy reveals isosbestic points (vide infra), thus confirming that no long-lived intermediates are formed. This observation is in agreement with a recent study of the Strating−Zwanenburg photobisdecarbonylation of **7** by time-resolved spectroscopy.[54]

B. UV/vis Spectroscopy of Higher Acenes. General. The UV/vis spectra of the smaller members of the acene series and benzene have been thoroughly investigated previously.[1,31,55−61] Comparison with the higher members is instructive and is briefly summarized here. The electronic absorption spectra of the acenes are dominated by three major transitions, which were named p, α, and β by Clar[1] and ^1L_a, ^1L_b, and ^1B_b, respectively, by Platt.[57] While the Platt nomenclature describes excited states, Clar's terminology, which we use for the remainder of the paper, focuses on the electronic transitions. The α and β bands originate from transitions that are polarized along the long molecular axis and thus correspond to excitations from the ground state into states of B_{3u} symmetry (covalent $^1B_{3u}^-$ and ionic $^1B_{3u}^+$, respectively, using Pariser's alternancy symmetry). The p transition is polarized along the short axis and results from excitation into a state of B_{2u} symmetry ($^1B_{2u}^+$). The α bands usually are the weakest ($\log \varepsilon \approx 2-3$), followed by the p bands ($\log \varepsilon = 4$), and the β bands are the strongest absorptions ($\log \varepsilon \approx 4-6$) in the spectra.[1]

Though not an acene in the strict sense, benzene can be considered the parent of the acene series. Because of its higher D_{6h} symmetry, the α and p transitions of benzene are electric dipole forbidden, while the β transition is dipole allowed. The α and p transitions are nonetheless observed with medium intensity ($\log \varepsilon \approx 3$) due to vibronic coupling. The longest wavelength absorption is due to the α transition, followed by p and β transitions with increasing energy. All three transitions shift to the red upon linear annelation, but the p band shifts faster than the α band. The longest wavelength absorption is still the α band in naphthalene, but already for anthracene it is the p band. Due to the vibronic fine structure and the higher intensity of the p band in the acene series, the α band is obscured for anthracene and tetracene. It is again discernible in pentacene. At least one additional band is observed to the red of the β band for tetracene, pentacene, and hexacene.[58−60] On the basis of polarization measurements for tetracene,[59] Tavan and Schulten[17] assigned this absorption to arise from an excitation into the $2^1B_{3u}^-$ state. This assignment was later supported for tetracene in a multireference perturbation theory (MRMP) study.[19]

Using CC2 theory, Grimme and Parac found reasonable agreement with experiment for the energies of the p and α bands of acenes.[23] We have previously computed the excited states of heptacene at the RICC2 level,[45] but additional computations (see Supporting Information for details) and comparison with experimental and MRMP data for tetracene suggest that some of the higher excited states are not well described by CC2 theory. We thus limit the comparison of experiment and theory to the p, α, and β bands.

Pentacene. The photodecomposition of the dione **5** yields pentacene which is characterized by p and β bands at 562 and 292 nm, respectively (see Figure 1 and Table 1). The data are in good agreement with previous investigations in solution and with the data of Halasinski et al.[61] in solid argon (559.8 and 291.2 nm, respectively). This shows that the inevitable presence of CO in the vicinity of the photogenerated pentacene molecules in our experiments does not have a significant effect on the spectral properties of the acene.

In addition to the bands observed in a previous matrix isolation study by Halasinksi et al.,[61] absorptions in the 400−430 nm range are clearly observed in our experiments. We assign the band at 422 nm to the α transition from the ground to the 1^1B_{3u} state in pentacene. This transition is blue-shifted by 9 nm (500 cm^{-1}) compared to the value measured in a cyclohexane−benzene (9:1) mixture at room temperature.[58] We thus obtain $\nu_\beta:\nu_\alpha = 1.45$, which lies within the range typically observed for this

(49) Becke, A. D. *J. Chem. Phys.* **1993**, *98*, 5648.
(50) Lee, C.; Yang, W.; Parr, R. G. *Phys. Rev. B* **1988**, *37*, 785.
(51) Frisch, M. J. et al. Gaussian 03, Revision B.4, Pittsburgh, PA, 2003.
(52) Merrick, J. P.; Moran, D.; Radom, L. *J. Phys. Chem. A* **2007**, *111*, 11683.
(53) Givan, A.; Loewenschuss, A.; Nielsen, C. J. *J. Chem. Soc., Faraday Trans.* **1996**, *92*, 4927.
(54) Mondal, R.; Okhrimenko, A. N.; Shah, B. K.; Neckers, D. C. *J. Phys. Chem. B* **2008**, *112*, 11.
(55) Clar, E. *Ber. Dtsch. Chem. Ges.* **1936**, *69*, 607.
(56) Clar, E. *Chem. Ber.* **1949**, *82*, 495.
(57) Klevens, H. B.; Platt, J. R. *J. Chem. Phys.* **1949**, *17*, 470.
(58) Nijegorodov, N.; Ramachandran, V.; Winkoun, D. P. *Spectrochim. Acta A* **1997**, *53*, 1813.
(59) Bree, A.; Lyons, L. E. *J. Chem. Soc.* **1960**, 5206.
(60) Perkampus, H.-H. *UV-VIS Atlas of Organic Compounds*; 2nd ed.; VCH: Weinheim, 1992.
(61) Halasinski, T. M.; Hudgins, D. M.; Salama, F.; Allamandola, L. J.; Bally, T. *J. Phys. Chem. A* **2000**, *104*, 7484.

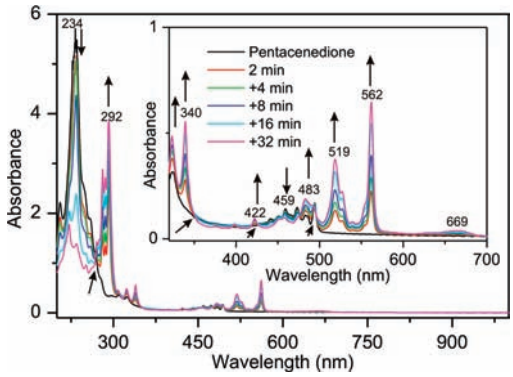

Figure 1. Electronic absorption spectra measured in solid argon (10 K) during the photodecomposition ($350 \leq \lambda \leq 450$ nm) of α-diketone **5**. Inset: Enlargement of the 320−700 nm region. Vertical arrows pointing downward and upward indicate decrease and increase of the absorption during photolysis. The diagonal arrows at 269, 352, 476, and 499 nm mark isosbestic points.

Table 1. Experimental Electronic Transition Energies and Intensities for Pentacene (**2**) in Solid Inert Gas Matrices at 10 K

	Ar			Xe
band system	λ_{max} (nm)[a]	ω (eV)	abs	λ_{max} (nm)[a]
VI.	**221**	5.61	0.44	-
V.	**251**	4.94	0.23	-
	281	4.41	0.79	289
	286	4.34	0.75	295
IV. β, (^1B_b)	**292**	4.25	1.00	**301**
	307	4.04		-
	324	3.83	0.12	329
III.	**340**	3.65	0.14	**345**
	399	3.11	0.02	-
II. α (^1L_b)	**422**	2.94	0.03	-
	458	2.71	0.03	461
	483	2.57	0.05	495
	519	2.39	0.10	531
	527	2.35	0.06	539
I. p (^1L_a)	**562**	2.21	0.18	**576**
aggr	669	1.85	-	-

[a] The lowest energy bands within a system are given in bold print.

ratio in polycyclic aromatic compounds.[62] The energy computed for the 1^1B_{3u} state (3.24 eV) at the RICC2 level is too high by 0.3 eV compared to experiment (2.94 eV).[23]

The band system with the strongest absorption at 340 nm (3.65 eV) shows vibrational fine structure, in agreement with the data of Halasinski et al.[61] In benzene solution, a band at 350 nm and a shoulder to the red of the β band at 330 nm are observed, and these were assigned previously to arise from the $2^1B_{3u}^-$ and $2^1B_{2u}^+$ states, respectively, by Tavan and Schulten.[17] The shape observed here suggests that the system is associated with one excited state only, presumably $2^1B_{3u}^-$ based on comparison with tetracene.

In addition, a broad peak appeared at around 669 nm during the photogeneration of pentacene in an argon matrix. This peak started forming only after a significant amount of pentancene was produced in the matrix, which can be safely assigned to the aggregated state of pentacene. Spontaneous aggregation of pentacene is well-known on SiO_2 and gold surfaces[63,64] but should be precluded under matrix isolation conditions.

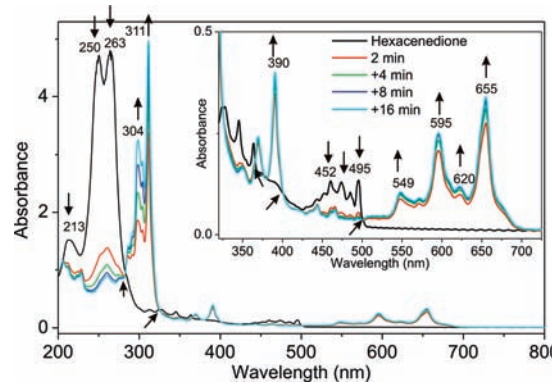

Figure 2. Electronic absorption spectra measured in solid argon (10 K) during the photodecomposition ($350 \leq \lambda \leq 450$ nm) of α-diketone **6**. Inset: Enlargement of the 320−725 nm region. Vertical arrows pointing downward and upward indicate decrease and increase of the absorption during photolysis. The diagonal arrows at 284, 325, 365, 401, and 501 nm mark isosbestic points.

Table 2. Experimental Electronic Transition Energies and Intensities for Hexacene (**3**) Measured in Solid Inert Gas Matrices at 10 K

	Ar			Xe
band system	λ_{max} (nm)[a]	ω (eV)	Abs.	λ_{max} (nm)[a]
	298	4.16	0.53	308
	304	4.08	0.43	314
IV. β, (^1B_b)	**311**	3.99	1.00	399
	350	3.54		-
	369	3.36	0.03	376
III.	**390**	3.18	0.04	399
II. α (^1L_b)	overlaps with precursor			
	549	2.26	0.01	531
	595	2.08	0.002	-
	620	2.00	0.01	613
I. p (^1L_a)	**655**	1.89	0.03	**673**

[a] The lowest energy bands within a system are given in bold print.

Hexacene. The UV/vis spectrum of hexacene (see Figure 2 and Table 2) displays the expected bathochromic shift of the p and β bands to 655 and 311 nm, respectively. The values are in good agreement with the data of Nijegorodov et al.,[58] who measured 14500 cm^{-1} (690 nm) and 31600 cm^{-1} (316 nm), respectively, in cyclohexane−benzene (9:1) solution. Assuming at least a similar error for the α band as in pentacene (0.3 eV), the corrected theoretical value for hexacene is around 2.79 eV or 444 nm.[23] This is in good agreement with the data of Nijegorodov et al.,[58] who gave the α band at 22700 cm^{-1} (440 nm). In our experiment there are absorptions in the 430−470 nm range that we cannot assign unambiguously to hexacene, as the precursor also absorbs in this range. As observed in pentacene, there is a band system between the expected location of the α band and the β band. Its most intense absorption is at 390 nm, and it features a vibrational progression with a spacing of 1460 cm^{-1}. This band system is bathochromically shifted by 50 nm compared to its value of 340 nm in pentacene.

Heptacene. Except for our own preliminary reports of the heptacene UV/vis spectrum,[44,45] experimental data for heptacene are not available. As expected, the electronic absorptions are further bathchromically shifted in heptacene (Figure 3 and Table 3). The intense β band is now located at 326 nm. The theoretical excitation energy (3.89 eV; RICC2/TZVPP, see Table

(62) Zander, M. *Polycyclische Aromaten*; B. G. Teubner: Stuttgart, 1995.
(63) Yoshikawa, G.; Sadowski, J. T.; Al-Mahboob, A.; Fujikawa, Y.; Sakurai, T.; Tsuruma, Y.; Ikeda, S.; Saiki, K. *Appl. Phys. Lett.* **2007**, *90*, 251906.
(64) Menozzi, C.; Corradini, V.; Cavallini, M.; Biscarini, F.; Betti, M. G.; Mariani, C. *Thin Solid Films* **2003**, *428*, 227.

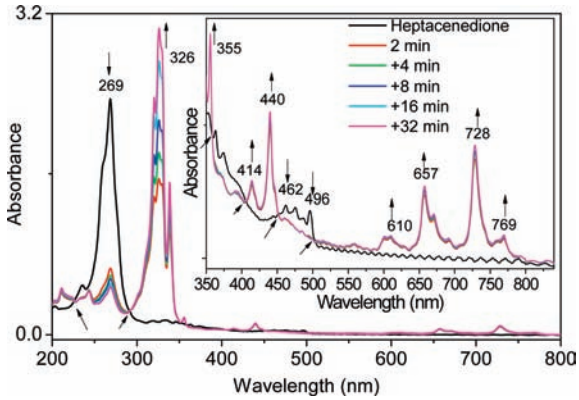

Figure 3. Electronic absorption spectra measured in solid argon (10 K) during the photodecomposition ($350 \leq \lambda \leq 450$ nm) of α-diketone **7**. Inset: Enlargement of the 350−850 nm region. Vertical arrows pointing downward and upward indicate decrease and increase of the absorption during photolysis. The diagonal arrows at 226, 291, 358, 407, 452, and 503 nm mark isosbestic points.

Table 3. Experimental Electronic Transition Energies and Intensities for Heptacene Measured in Solid Gas Matrixes at 10 K

	Ar			Xe
band system	λ_{max} (nm)[a]	ω (eV)	int	λ_{max} (nm)[a]
	320	3.88	0.77	326
	326	3.80	1.00	-
VI. β, (^1B_b)	**329**	3.77	0.93	**335**
V.	**338**	3.66	0.46	**347**
IV.	**355**	3.49	0.05	**362**
	388	3.20		-
	414	2.99	0.02	422
III.	**440**	2.82	0.04	**448**
II. α (^1L_b)		not observed		
	559	2.22	0.004	568
	601	2.06	0.006	617
	610	2.03	0.01	626
	657	1.89	0.02	676
	670	1.85	0.01	706
	690	1.80	0.005	721
	704	1.76	0.003	752
I. p (^1L_a)	**728**[b]	1.70	0.03	**776**[b]
	769[b]	1.61	0.006	787[b]

[a] The lowest energy bands within a system are given in bold print. [b] See section B for details.

S3) is in remarkably good agreement with experiment (3.80 eV) considering the size of the system. The strongest absorption of the p band system is observed at 728 nm and thus the error in the computed transition energy (1.53 eV vs 1.70 eV from experiment, see Table S3) is increasing with acene length. This is in agreement with the theoretical analysis given by Grimme and Parac.[23]

Based on the data of pentacene and hexacene, the α band is expected at around 470 nm or possibly at even slightly longer wavelengths assuming again an error of at least 0.3 eV in the computed absorption energy (see Supporting Information). However, in this range the photoprecursor absorbs and in view of the expected weakness of the α band no signal can be unambiguously assigned in the expected range to the α band.

Also in heptacene the band system with the vibrational progression is observed between the β and the expected location of the α band. Its most intense absorption is shifted to 440 nm, and the spacing is reduced to 1427 cm^{-1}.

Two additional bands are observed between this band system and the β band: one weak band at 355 nm and one rather intense

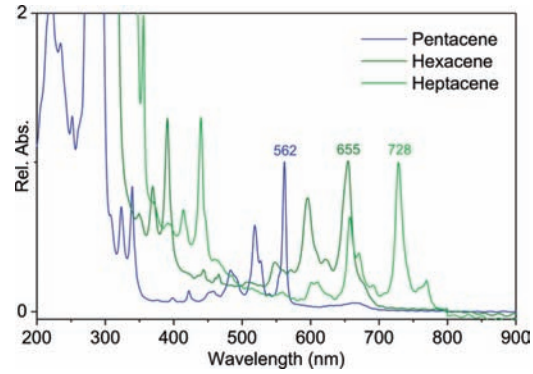

Figure 4. Comparison of the electronic absorption spectra of the acenes studied in the present work. The spectra were obtained from the photoprecursors **5**−**7** in argon matrices at 10 K.

one at 338 nm. The origin of these bands is not clear to us at this time. But we note that Sony and Shukla[26] have computed a rather intense band to the red of the β band using a multireference configuration interaction (MRCISD) approach in conjunction with a screened semiempirical PPP Hamiltonian. The difference given by these authors between this "new" intense band and the β band of 14 nm is in good agreement with the 12 nm observed in the experiment.

Comparison of the UV Spectra of Higher Acenes. We have so far not discussed the details of the p band observed in heptacene (Figure 4). In the acene series up to hexacene[58] the most intense transition in the p band system is the 0−0 absorption which is thus also the longest wavelength feature of the acenes beyond naphthalene. There is no obvious reason that this should differ for the acenes beyond hexacene. In heptacene, however, we observe a longer wavelength absorption of lower intensity at 769 nm. This is also the case if the heptacene is generated at room temperature in a PMMA matrix.[65] Close inspection of the hexacene p band reveals a shoulder at longer wavelength than the 0−0 transition in our experiment, but this shoulder is absent in solution.[36,58] One explanation for these longer wavelength features in hexacene and heptacene are deviations from the expected planarity due to the constraints imposed by the matrix host. The dihedral angles between the acene subunits in the photoprecursors are close to 120°, and these need to open up to 180° in the acene. It cannot be excluded that the rigid matrix precludes achieving planarity for some molecules, and for these distorted species, longer wavelength absorptions are expected than for the equilibrated molecules. Because of its larger size, this effect is expected to be more pronounced for heptacene than for hexacene and is obviously absent for pentacene.

Note that similar features at longer wavelengths are not observed for the radical ions even though they should also be expected if they originate from matrix effects. Also, annealing samples of heptacene generated at 10 K in argon up to 30 K did not change the UV spectra. Likewise, photogeneration of heptacene at 30 K rather than at 10 K produced identical spectra. For small molecules, these techniques usually allow geometrical relaxation and identification of unstable matrix sites, but for the large heptacene the available thermal energy might not suffice to allow the structural equilibration of the molecules. Unambiguous proof that the long wavelength bands in the p

(65) Mondal, R.; Shah, B. K.; Neckers, D. C. *J. Org. Chem.* **2006**, *71*, 4085.

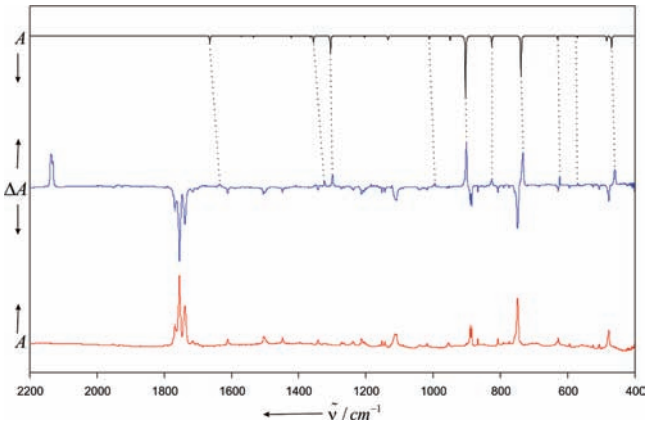

Figure 5. Mid-IR spectra (Ar, 10 K) of the photochemical decomposition of **5** and formation of pentacene. Bottom: IR spectrum of **5** obtained after deposition for 50 min at 163 °C. Middle: difference spectrum after 18 h of irradiation ($385 < \lambda < 450$ nm); bands pointing downward decrease during irradiation, those pointing upward increase. Top: IR spectrum computed for **2** at the RB3LYP/6-31G* level scaled by 0.985.

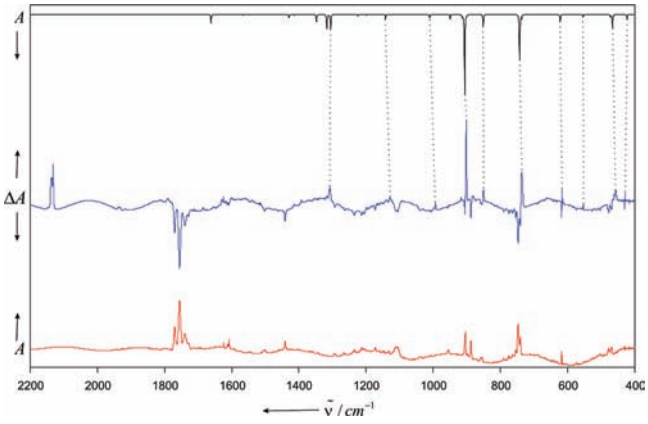

Figure 6. Mid-IR spectra (Ar, 10 K) of the photochemical decomposition of **6** and formation of hexacene. Bottom: IR spectrum of **6** obtained after deposition for 75 min at 195 °C. Middle: difference spectrum after 2.5 h of irradiation ($385 < \lambda < 450$ nm); bands pointing downward decrease during irradiation, those pointing upward increase. Top: IR spectrum computed for **3** at the RB3LYP/6-31G* level scaled by 0.985.

band systems of heptacene (and the p band of hexacene) are either due to incomplete relaxation of the molecules or are an intrinsic feature of the electronic structure of heptacene should be possible by generation of the acene in the gas phase before being trapped by an excess of argon under cryogenic conditions so that the molecules would have sufficient time to relax to their equilibrium geometries. Such experiments are currently not feasible with our equipment but are planned for the future.

It is noteworthy that the weak band that first appears to the red of the β band of tetracene at 289 nm (see Supporting Information) is shifting bathochromically by an almost constant increment of 50 nm per additional ring and thus arrives at 440 nm for heptacene. We currently cannot determine the nature of this state, but following previous computational and experimental investigations of the electronic absorption spectra of tetracene,[17,19] we tentatively assign it to the $2^1B_{3u}^-$ state. Future experimental investigations using polarized light should substantiate this assignment.

C. IR Spectroscopy of Higher Acenes. The mid-IR spectra of the acenes obtained in solid argon at 10−15 K do not provide as much information as do the electronic absorption spectra

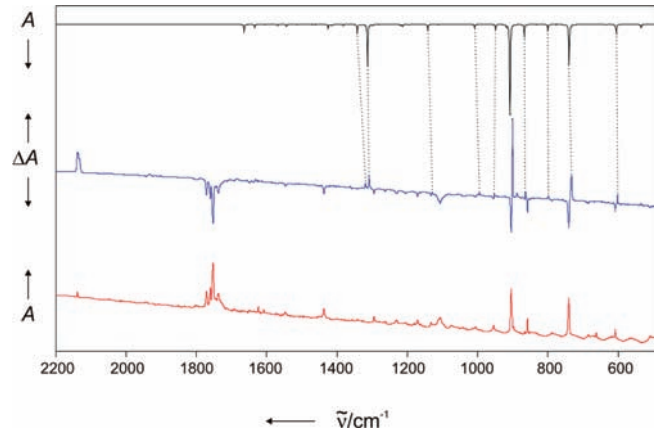

Figure 7. Mid-IR spectra (Ar, 10 K) of the photochemical decomposition of **7** and formation of heptacene. Bottom (blue): IR difference spectrum after 2.5 h of irradiation ($385 < \lambda < 450$ nm); bands pointing downward decrease during irradiation and those pointing upward increase. Middle (black): IR spectrum of **7** obtained after deposition for 75 min at 195 °C. Top (red): IR spectrum computed for **4** at the RB3LYP/6-31G* level of theory scaled by 0.985.

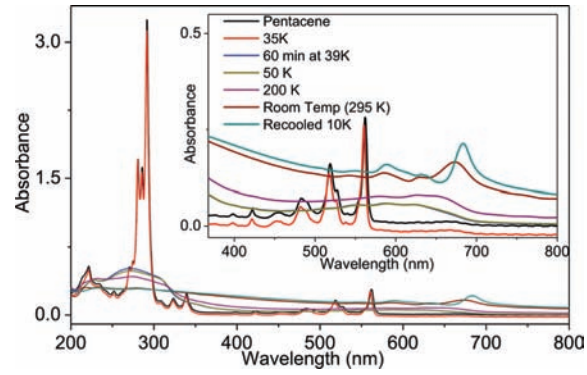

Figure 8. Annealing of pentacene photogenerated from α-diketone **5** in an argon matrix.

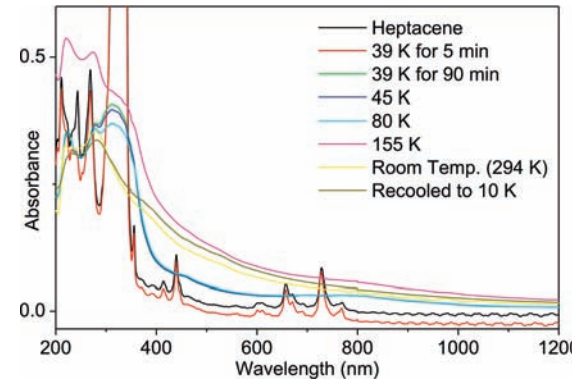

Figure 9. Annealing of heptacene photogenerated from α-diketone **7** in an argon matrix.

(Figures 5–9, and Tables S4−S6 for measured vibrational frequencies). The spectra are dominated by two strong absorptions around 900 cm^{-1} and 730 cm^{-1} due to out-of-plane deformations, γ_{CH}. They hardly are affected by the size of the acene: pentacene (901 cm^{-1}; 733 cm^{-1}), hexacene (902 cm^{-1}, 737 cm^{-1}), to heptacene (901 cm^{-1}, 741/733 cm^{-1}). This is in agreement with the theoretical analysis at the RB3LYP/6-31G* level of theory using a scaling factor of 0.985: 904, 906, and

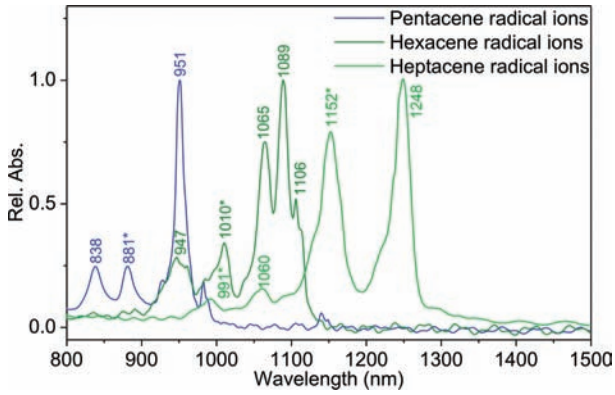

Figure 10. NIR absorptions of the radical ions photogenerated in solid argon at 10 K from pentacene, hexacene, and heptacene using UV irradiation (185 nm). Bands marked with an asterisk belong to the radical anion species.

903 cm^{-1} and 740, 743, and 740 cm^{-1} for pentacene, hexacene, and heptacene, respectively.

Another deformation mode involving the out-of-plane movement of both hydrogen and carbon atoms is found in the 450−475 cm^{-1} region. This band is always split and appears at 458.5/460 cm^{-1}, 457/460 cm^{-1}, and 461/468 cm^{-1} for the three acenes with increasing size.

A further characteristic for the acenes is a doublet in the 1300−1325 cm^{-1} region which is due to modes of b_{1u} and b_{2u} symmetry having in-plane deformation character involving both C−H and C−C bonds. The bands move closer with acene size: 1323/1300 cm^{-1} in pentacene and 1319/1309 cm^{-1} in heptacene. There are two modes of b_{1u} symmetry of similar intensity predicted for hexacene (1318 and 1306 cm^{-1}), but only one split band is observed (1310/1307 cm^{-1}). The b_{2u} symmetry mode is shifted to 1348 cm^{-1} according to theory but not observed experimentally.

As discussed by Bendikov et al.,[24] the RB3LYP/6-31G* solution has a triplet instability for heptacene and a lower energy solution can be obtained by using spin-unrestricted theory, i.e., UB3LYP/6-31G*. The vibrational spectrum obtained at the UB3LYP/6-31G* level of theory agrees well with the RB3LYP/6-31G* one with respect to transition energies but differs somewhat with respect to the intensities (see Supporting Information, Figure S2). The RB3LYP spectrum is found to be in better agreement with experiment, in particular in the 1600−1200 cm^{-1} region, and is thus displayed in Figure 7.

D. Stability of Higher Acenes. Thermal stabilities of **2**−**4** were evaluated by carefully evaporating the matrix host gas and monitoring the changes in the UV−vis−NIR absorption spectra. The host gas, argon, evaporates slowly at 39−40 K under our experimental conditions. Pressure increases to 10^{-4} mbar during evaporation, and the pressure decreases to 10^{-6} mbar after argon gas is completely evaporated. During the annealing experiment of pentacene (Figure 8), the spectral feature does not change except for shifting the baseline at temperatures up to 39 K. However, beyond this temperature when the argon gas is completely evaporated, the structured band of **2** disappeared, and a ∼50−60 nm red-shifted broadband absorption was observed. Interestingly, this band progressed slowly toward red with time and temperature, and finally, after standing overnight at room temperature, the absorption spectra became more structured and resembled the reported solid-state absorption spectra of **2**.[66,67] The broad absorption in between solution and solid state indicates an aggregated state of **2**, which slowly equilibrates to the solid-state packing via $\pi-\pi$ interaction. Further cooling of the remaining compound to 10 K does affect the molecular packing of **2** as indicated by the absorption spectra. The absorption spectra of **2** at 10 K became more narrow and ∼10 nm red-shifted from the spectra recorded at room temperature. A similar red-shifted aggregated state followed by the solid-state packing was observed during the annealing experiment of hexacene, and the changes in the absorption spectra are shown in Figure S3.

In the case of heptacene, the intermediate aggregated state was observed up to ∼80 K. However, no absorption in the region of 750−1000 nm was observed beyond 155 K (Figure 9). The UV spectrum of remaining material, a heptacene dimer of unknown constitution according to LDI-TOF, has a band at 280 nm and does not show any changes upon warming to room temperature or cooling to 10 K. These experiments indicate that heptacene is not stable if it is not protected from dimerization by the matrix. Heptacene behaves like its smaller analogues up to an intermediate temperature, such as 80 K, and shows an aggregated state ∼ 800 nm. However, at higher temperature the molecules of **4** come sufficiently close to collapse by dimerization. This unexpectedly fast reaction of **4** surely is related to its high diradical character,[24,27] which obviously results in a very low barrier for the dimerization reaction.

Earlier we attempted to synthesize heptacene following a classical Meerwein−Ponndorf−Verley (MPV) reduction of 7,16-heptacenequinone, which yielded a brownish final product.[68] The ^{1}H NMR spectrum (Figure S4) of the product in DMSO-d_6 revealed several protons in the aliphatic region, especially about ∼5.4 ppm along with multiple peaks in the aromatic region. This can be explained by formation of a mixture of dimers immediately after heptacene is produced in the reaction mixture. Overreduction of heptacene to form di- or tetra-hydroheptacene also cannot be ruled out. Purification of the mixture was unsuccessful because of its lack of solubility, and vacuum sublimation was also unsatisfactory. In 1986, Fang also attempted to synthesize molecular heptacene and arrived at similar conclusions.[69]

E. Photoionization of Higher Acenes. Irradiation of the acenes with the output of a low pressure mercury lamp that emits mainly at 254 nm, but also somewhat at 185 nm, results in the photoionization of the acene molecules. Both the radical anion and the radical cation can be observed simultaneously in the argon matrix because of photoinduced charge separation. By use of an appropriate cutoff filter (220 nm), it can be shown that only the 185 nm line is responsible for the photoredox reaction. Visible light irradiation results in quick collapse of the charged species to the neutral acenes.

The acene radical ions show very characteristic absorptions in the NIR region between 800−1250 cm^{-1} (Figure 10) and in the visible region in the 400−480 nm range. As expected, these absorptions shift bathochromically with acene size. Doping of

(66) Herwig, P. T.; Müllen, K. *Adv. Mater.* **1999**, *11*, 480.
(67) Hinderhofer, A.; Heinemeyer, U.; Gerlach, A.; Kowarik, S.; Jacobs, R. M. J.; Sakamoto, Y.; Suzuki, T.; Schreiber, F. *J. Chem. Phys.* **2007**, *127*, 194705.
(68) Mondal, R. Synthesis and Study of Higher Poly(acene)s: Hexacene, Heptacene, and Derivatives, Ph.D. Thesis, Bowling Green State University, Bowling Green, OH, 2007.
(69) Fang, T. Heptacene, Octacene, Nonacene, Supercene and Related Polymers, Ph.D. Thesis, University of California, Los Angeles, CA, 1986.

Table 4. Experimental and Computed (TD-UB3LYP/6-31G*//UB3LYP/6-31G*) Transition Wavelengths (λ in nm) and Oscillator Strengths for Pentacene Radical Ions Photogenerated by 185-nm Irradiation

pentacene radical cation, X^2B_{3g}					pentacene radical anion, X^2B_{1u}				
state	Ar, 10 K	Xe, 10 K	theory	*f*	state	Ar, 10 K	Xe, 10 K	theory	*f*
3^2B_{1u}	324	325	399	0.021	3^2B_{2g}	not obsd	not obsd	372	0.010
	340	345			2^2B_{3g}	not obsd	not obsd	410	0.003
2^2B_{1u}	not obsd	not obsd	435	0.013	2^2B_{2g}	not obsd	not obsd	421	0.089
2^2A_u	423	426	442	0.120		795	not obsd		
	750	not obsd			1^2B_{2g}	881	881	750	0.260
	839	840							
	928	not obsd							
1^2A_u	951	952	821	0.229	1^2B_{3g}	not obsd	not obsd	1049	0.013
1^2B_{1u}	982	989	987	0.012					
aggr	1140	-							

Table 5. Experimental and Computed (TD-UB3LYP/6-31G*//UB3LYP/6-31G*) Transition Wavelengths (λ in nm) and Oscillator Strengths for Hexacene Radical Ions Photogenerated by 185-nm Irradiation

hexacene radical cation, X^2A_u					hexacene radical anion, X^2B_{2g}				
state	Ar, 10 K	Xe, 10 K	theory	*f*	state	Ar, 10 K	Xe, 10 K	theory	*f*
2^2B_{3g}	453	454	471	0.165					
	947	broad	-	-	-	890	broad		
	1065	1069	-	-	1^2B_{1u}	1010	-	844	0.348
1^2B_{3g}	1089	1097	920	0.306					
1^2B_{2g}	1557	-	1357	0.010	1^2A_u	not obsd		1464	0.011

Table 6. Experimental and Computed (TD-UB3LYP/6-31G*//UB3LYP/6-31G*) Transition Wavelengths (λ in nm) and Oscillator Strengths for Heptacene Radical Ions[a]

heptacene radical cation, X^2B_{3g}					heptacene radical anion, X^2B_{1u}				
state	Ar, 10 K	Xe, 10 K	theory	*f*	state	Ar, 10 K	Xe, 10 K	theory	*f*
3^2B_{1u}	not obsd		491.4	0.002	2^2B_{2g}	472	489	466.0	0.151
2^2A_u	480		495.9	0.217	3^2B_{3g}	not obsd		474.2	0.001
2^2B_{1u}	not obsd		628.9	0.000	2^2B_{3g}	not obsd		604.6	0.000
	1060	1081							
	1087	1109				991	1006		
1^2A_u	1248[b]	1274	1023.9	0.391	1^2B_{2g}	1152	1179	942.2	0.445
1^2B_{1u}	2134	2179	1908.3	0.009	1^2B_{3g}	not obsd		2101.4	0.009

[a] For comparison of the spectra obtained in argon and xenon, see Figure S5. [b] Most intense band within a system.

the matrix with CH_2Cl_2, a better electron acceptor than the acene, suppresses formation of the acene radical anion and allows the assignment of the transitions to either the radical anion or the radical cation of the respective acene. In this way, the yield of the radical cation in the photoreaction can also be increased.

Pentacene Radical Ions. Halasinksi et al.[61] reported a detailed analysis of the spectra of the radical cation and anion of pentacene. The most intense absorption at 951 nm (lit. 955 nm) is due to the radical cation and corresponds to the 0−0 transition of the $X^2B_{3g} \rightarrow 1^2A_u$ (i.e., SOMO → LUMO) excitation. Three weaker features at longer wavelengths (985, 967, and 962 nm) were assigned to the $X^2B_{3g} \rightarrow 1^2B_{1u}$ (i.e., SOMO-1 → SOMO) transition.[61] In our experiment (Table 4) these three features are not resolved. Instead we observe a band at 982 nm. For the pentacene radical anion, also two transitions were tentatively assigned by Halasinksi et al.,[61] namely the weaker $X^2B_{1u} \rightarrow 1^2B_{3g}$ (SOMO-1 → SOMO) transition at 908 nm and the stronger $X^2B_{1u} \rightarrow 1^2B_{2g}$ (SOMO → LUMO) transition at 882 nm. In our experiment we can clearly observe the 881 nm transition only.

Hexacene Radical Ions. Previous experimental investigations of hexacene radical ions are limited to the work of Angliker et al.[70] who characterized both the cation and anion by ESR spectroscopy and also measured the electronic absorption spectrum of the anion. The authors identified seven band systems in the range 300−2000 nm. The longest wavelength absorption extends to almost 1800 nm and was assigned to the $X^2B_{2g} \rightarrow 1^2A_u$ transition by Angliker et al.,[70] in agreement with TD-DFT data at the BLYP/6-31+G*//BLYP/6-31+G* level (0.78 eV, ≈1590 nm) reported by Malloci et al.[28] and our own computations (Table 5). This band system is not observed in our experiment, presumably because of its low intensity. The second band system, ($X^2B_{2g} \rightarrow 1^2B_{3u}$), is around 1000 nm in the experiment of Angliker et al.[70] The TD-DFT value for this transition is higher, 1.34 eV (925 nm) at TD-BLYP,[28] and still higher at our standard level, i.e., B3LYP/6-31G*. In our experiments, we observe this transition at 1010 nm.

The electronic absorption spectrum of the hexacene radical cation is not known. We observe a band system with the strongest feature at 1089 nm and assign this to the $X^2A_u \rightarrow 1^2B_{3g}$ (SOMO → LUMO) transition, in agreement with TD-DFT computations. The SOMO-1 → SOMO transition ($X^2A_u \rightarrow 1^2B_{2g}$) is observed at 1557 nm, in agreement with theory (TD-BLYP: 0.84 eV, 1476 nm; TD-B3LYP: 1357 nm).[28] Another transition observed in the experiment is at 453 nm, and this is assigned to $X^2A_u \rightarrow 2^2B_{3g}$. The Coulson−Rushbrooke pairing theorem demands very similar electronic absorption spectra for radical anions and cations for alternant hydrocarbons

(70) Angliker, H.; Gerson, F.; Lopez, J.; Wirz, J. *Chem. Phys. Lett.* **1981**, *81*, 242.

and indeed the corresponding transition is observed at around 450 nm by Angliker et al.[70] for the radical anion but not in our experiment.

Heptacene Radical Ions. The electronic absorptions of the radical ions of heptacene are further shifted bathochromically (Figures 10 and S5). For the radical cation the SOMO-1 → SOMO transition is bathochromically shifted to 2134 nm, while the SOMO → LUMO transition is observed at 1248 nm (Table 6). As with the radical anions of the smaller acenes, the SOMO-1 → SOMO transition cannot be observed in our experiment because of its small intensity. The SOMO → LUMO transition is bathochromically shifted with respect to hexacene radical anion but at shorter wavelength as the corresponding transition in the radical cation. This is in agreement with all other acene radical ions discussed above.

Conclusions

The synthesis of the three highest known acenes, pentacene (**2**), hexacene (**3**), and heptacene (**4**), was achieved under the conditions of matrix isolation using the Strating−Zwanenburg reaction, the photochemical bisdecarbonylation of bridged α-diketones. This approach to the synthesis of higher acenes allows the investigation of the spectral properties and the thermal stabilities of these important oligoacenes under identical conditions and the study of the influence of the conjugation length on the electronic structures. Furthermore, photoexcitation of the acenes **2**−**4** using the output of a low pressure mercury lamp (λ = 185 nm) results in the electron transfer between acene molecules and concurrent formation of radical cation and anions in the matrix. This photoinitiated redox reaction can be reversed by visible light irradiation. More specifically, the following conclusions can be drawn from this work:

1. The photobisdecarbonylation of the α-diketones is nearly quantitative and produces no intermediates detectable on a nanosecond or longer time scale. This approach thus should be a robust method for the synthesis of acenes.

2. The features of acenes in the electronic absorption spectra arising from the p, α, and β bands shift to longer wavelength as expected. The ambiguity with respect to the location of the α band in pentacene could be resolved: in agreement with older literature, the α band is observed around 420 nm.

3. Heptacene shows an unexpected absorption to the red of the 0−0 transition of the p band, while for hexacene only a shoulder can be observed. While such longer wavelength absorptions have also been observed for the substituted heptacenes,[41,42] their origin is not clear at this time. Under our matrix isolation conditions, the formation of J-aggregates appears unlikely. Deviation from the expected high symmetry due to impeded relaxation from the kinked geometry of the α-diketone photoprecursor in the rigid matrix environment cannot be ruled out. Unless this feature is intrinsic to the higher acenes, this is in our judgment the most likely reason for the long wavelength absorptions in our experiment.

4. As expected, the IR spectra of oligoacene are similar and dominated by deformation modes. It is noteworthy that the experimental IR spectra agree well with those computed at the RB3LYP/6-31G* level of theory. The spin-unrestricted (UB3LYP/6-31G*) treatment, that is possible because of the triplet instability of the Kohn−Sham wave function identified by Bendikov et al.,[24] yields a computed IR spectrum that is in slightly poorer agreement with experiment.

5. The photochemically generated radical ions absorb strongly in the NIR region and show the expected bathochromic shift with system size. The SOMO → LUMO transitions are stronger than the lower energy SOMO-1 → SOMO transitions that extend up to 2134 nm for the heptacene radical cation in solid argon.

6. In contrast to pentacene and hexacene, heptacene is unstable at room temperature in a high vacuum system, even in the absence of oxygen. Careful evaporation of the argon matrix at $T < 40$ K and subsequent annealing of the remaining heptacene to room temperature reveals that the long wavelength absorption of heptacene disappears above ∼150 K. As the annealing process was followed by UV/vis spectroscopy, a photochemical reaction cannot be ruled out. But as this spectroscopy is the only one suitable under our experimental conditions, we are facing a dilemma with respect to the investigation of the stability of heptacene.

Acknowledgment. This work was supported in Bochum by the DFG (Heisenberg Fellowship) and the Fonds der Chemischen Industrie, and in Bowling Green by the Office of Naval Research, ONR N00014-06-1-0948 and the Ohio Department of Development. H.F.B. thanks Professor Wolfram Sander for interest and access to matrix isolation equipment, Dirk Grote for performing the ESR, Rolf Breuckmann for performing the LDI-TOF measurements, and Prof. Shukla for helpful discussions. R.M. thanks the McMaster Endowment (BGSU) for a research Fellowship.

Supporting Information Available: Infrared and electronic absorption data of **5**−**7**, infrared spectral data of acenes **2**−**4**, electronic absorption spectrum of tetracene (Ar, 10 K), UV/vis spectra of annealed hexacene, NMR spectra obtained upon photogeneration of heptacene in solution, computed excited state energies of naphthalene to heptacene at the RICC2/TZVPP//(U)B3LYP/6-31G* level of theory including computational details and Cartesian coordinates, and complete ref 51. This information is available free of charge via the Internet at http://pubs.acs.org/.

JA901841C